ISSN 1070-3632, Russian Journal of General Chemistry, 2015, Vol. 85, No. 3, pp. 689–691. © Pleiades Publishing, Ltd., 2015.

Structural, Optical, and Photocatalytic Properties of ZnS/α-Fe_2O_3 Core Shell Nano Particles[1]

Patij Shah, K. S. Siddhapara, and D. V. Shah

Department of Applied Physics, Sardar Vallabhbhai National Institute of Technology, Surat, 395007 India
e-mail: pks@svnit.ac.in

Received December 15, 2014

Abstract—Core shell ZnS/α-Fe_2O_3 nanoparticles were produced by the two-step method. In the first step uniform α-Fe_2O_3 particles were synthesized by hydrolysis of ferric chloride at 80°C. In the second step ZnS particles were added to α-Fe_2O_3 particles via hydrothermal rout at ca 90°C. The α-Fe_2O_3 and ZnS phases were identified by XRD and energy dispersive X-ray analysis (EDX). Crystal structure and morphology were studied by high resolution TEM. Photoreactivity of ZnS/α-Fe_2O_3 core shell nanoparticles was quantified by degradation of formaldehyde under UV irradiation.

Keywords: photoreactivity, two step method, core shell, pollutant degradation

DOI: 10.1134/S1070363215030287

INTRODUCTION

Recently semiconductor nano powders have been broadly studied in photocatalytic oxidation of organic and inorganic pollutants [1, 2]. Network structured nanocatalysts like SnO_2/ZnOTiO_2/Fe_2O_3 [3], mixed oxides [4], NiO/ZnO nanocomposites [5], and Cu_2O/TiO_2 hetero junction [6] demonstrated high photocatalytic activity. Nano powders are used as the coupled semiconductor photocatalytic materials though it is hard to recover those [7, 8].

Although the photocatalytic reactions rate can be increased significantly by noble metals but their large scale applications is not feasible because of high cost. Application of photocatalysis is limited by two major problems: recycling and low photoefficiency. A number of techniques is proposed for preparation of fixed photocatalytic systems to eliminate the first problem [9, 10]. In order to improve the photocatalytic activity of fine ZnS powders various approaches have been studied [11, 12]. In the current study we managed to develop (1) coating of magnetic Fe_2O_3 core by photoactive ZnS for magnetic photocatalysts and (2) easy recycling of the photocatalysts. After photodegradation the magnetic composites can be separated from the media by a simple magnetic process.

Zinc sulfide is an essential semiconductor [13] characterized by noticeable adaptability, the potential as light-emitting diodes (LEDs), sensors, application in flat panel displays, infrared windows and lasers. Its atomic structure and chemical properties are comparable with those of more extensively used ZnO. However, some properties of ZnS are more favorable than ZnO. To name a few, ZnS has a larger band gaps of 3.72 eV for cubic zinc blende (ZB) and 3.77 eV for hexagonal wurtzite (WZ) ZnS compared with ZnO (3.4 eV). Therefore ZnS is more applicable for visible-blind UV based devices such as sensors/photodetectors. ZnS is conventionally more favorable candidate for application in electroluminescence devices. However, the nanostructures of ZnS are studied to less extend than those of ZnO.

EXPERIMENTAL

Synthesis of zinc sulfide nanoparticles. Zinc sulfide nanoparticles were synthesized by adding sodium sulfide solution drop wise to zinc acetate solution. After 1 h of stirring of the solution a white precipitate of zinc sulfide was formed. In 24 h the mixture was washed with isopropyl alcohol and water to avoid agglomeration of particles. The precipitate was settled and dried in an oven over the period of 12 h at 90°C.

Synthesis of Fe_2O_3 nanoparticles. Uniform Fe_2O_3 particles were prepared by hydrolysis of ferric chloride at 80°C [6]. Stock solution of 3 M $FeCl_3$ and 0.2 M HCl were mixed in 1 : 3 ratio followed by addition of

[1] The text was submitted by the authors in English.

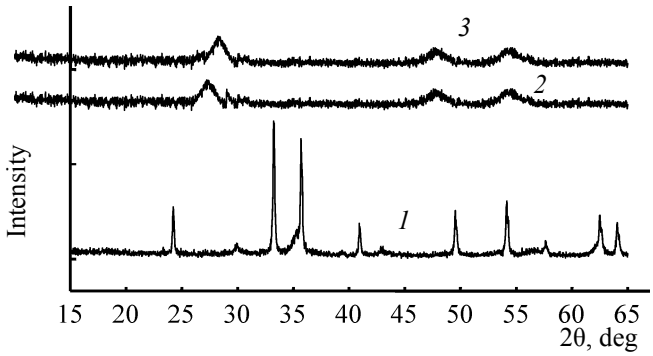

Fig. 1. XRD spectra of nanoparticles (*1*) Fe_2O_3, (*2*) ZnS/Fe_2O_3, and (*3*) ZnS.

deionized water to make the final concentration of Fe^{3+} equal to 0.01 M. The mixture was stored in a water bath at 96°C for 24 h, the residue filtered off and dried on a hot plate at 125°C to produce a dark brown fluffy precursor.

Synthesis of ZnS/α-Fe_2O_3 nanoparticles. The synthesized Fe_2O_3 (50 mg) was mixed with 40 mL of distilled water and ultrasonicated for 30 min. The sonicated Fe_2O_3 was added to 500 mL of distilled water and pH of the solution adjusted to 11.0 by NaOH (0.1 M) solution. Zinc acetate was added to Fe_2O_3 nanoparticles–distilled water system followed by dropwise addition of Na_2S upon continues stirring. In 24 h of stirring thus prepared product was washed repeatedly with distilled water and isopropyl alcohol and dried in an oven at 60°C for 6 h [7].

Characterization of products. XRD study of ZnS/α-Fe_2O_3 nanoparticles was performed by the Rigaku Miniflex-II Desktop XRD diffractometer coupled with a Cu X-ray tube, the CuK_α wavelength of which was selected by means of the nickel filter. EDAX was performed by Jeol SEM analyzer (Japan). Crystal structure and morphology of the products were studied by means of high resolution transmission electron microscopy (HRTEM, JEOL 2010). Photoluminescence measurements were carried out on a Fluorolog-3-Tau steady state lifetime spectrophotometer with a Xe lamp at room temperature.

Photocatalytic degradation of formaldehyde was carried out in a quartz reactor using a 250 V UV lamp.

RESULTS AND DISCUSSION

X-Ray diffraction (XRD). XRD patterns of the synthesized core shell nanoparticles are demonstrated in Fig. 1. The average crystalline size of the core shell particles ZnS, ZnS/Fe_2O_3, and Fe_2O_3 were 17.8, 20, and 14 respectively. Similarly, Shiet et al. [14], coated Ce doped TiO_2 in Fe_2O_3 nanoparticles. Formation of core shell is verified by the absence of reflections induced by Fe_2O_3 in the correspoding spectra. Spectra of ZnS/Fe_2O_3 demonstrated reflections similar to those of ZnS. Absence of any interactions between core and shell is also verified by the spectra. Except the spectrum of Fe_2O_3, all other peaks were broadened confirming nanonature of the particles.

The EDS spectrum of iron sulfide-iron oxide core shell particles indicated the presence of zinc, sulfur, iron and oxygen.

UV-Vis spectra. According to UV-Vis spectra light absorption was higher in case of coated nanoparticles [15] meaning that coated by ZnS nanoparticles could absorb a larger range of light radiation and increase the visible light absorption ability of photocatalysts.

Photocatalytic properties. Photoactivity of ZnS, ZnS/Fe_2O_3, and Fe_2O_3 catalysts in the same experimental environment is presented in Fig. 2. Without a catalyst no conversion of formaldehyde was observed. Conversion of formaldehyde induced by the particles upon 90 min of illumination reduced in the following order: $ZnS/Fe_2O_3 > ZnS > Fe_2O_3$ (Fig. 2). The photoactivity of ZnS, Fe_2O_3, and ZnS/Fe_2O_3 remained constant after 90 min of irradiation time, which was interpreted in terms of the large amount of byproducts attached to the surface of the catalysts that prohibited formaldehyde adsorption.

Although the surface adsorbed water and hydroxyl groups are essential for photocatalytic reactions [16], it is also clear that, among other factors, the nature of phase, surface area, capability of adsorption, and the surface acid–base properties [17] strongly influence the photoactivity. On the other hand, the experimental conditions such as mass of a catalyst, wavelength, temperature, radiant flux, initial concentration of the reactants, and oxygen pressure [18] can influence photo-activity of a catalysts. These parameters will be studied in our future work with ZnS, ZnS/Fe_2O_3, and Fe_2O_3 catalysts.

TEM. Transmission electron microscopy (TEM, JEOL 2010) was applied to the study of the crystal structure and morphology of the products. The average diameter and length of the core varied within the range 5–10 nm. The structure of the core shall remained the same as that of pure Fe_2O_3 core. The core shall

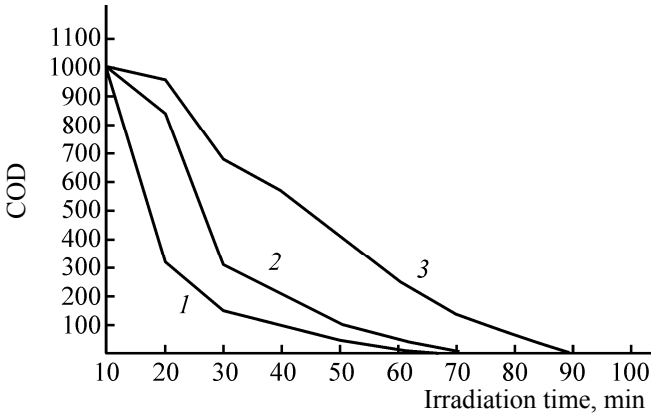

Fig. 2. Comparison of formaldehyde degradation: (*1*) ZnS/Fe_2O_3, (*2*) ZnS, and (*3*) Fe_2O_3.

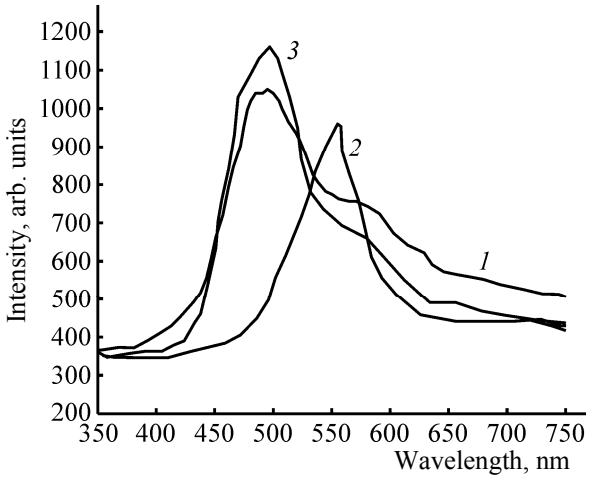

Fig. 3. Photoluminescence spectra of (*1*) ZnS/Fe_2O_3, (*2*) ZnS, and (*3*) Fe_2O_3.

nanoparticle dimensions varied from 10 nm to 15 nm. Coating of α-Fe_2O_3 nanoparticles resulted in formation of the core shell type structure, in which the core magnetite particles were coated very efficiently by the ZnS layer.

Photoluminescence. Photoluminescence (PL) spectra (270 nm excitation wavelength, room temperature) of ZnS/α-Fe_2O_3 core shell particles are presented in Fig. 3. The PL spectrum of ZnS exhibited one strong green emission peak at 492 nm and can be attributed to the self-activated centers formed by zinc vacancy in the ZnS lattice. The peak at 554 nm is characteristic to absorption by α -Fe_2O_3. It is noteworthy that at 492 nm the peak of α-Fe_2O_3/ZnS was of highest intensity.

CONCLUSIONS

Individual ZnS and Fe_2O_3 nanoparticles and ZnS/Fe_2O_3 core shell nanoparticles were efficiently synthesized by hydrolysis and characterized by XRD, UV-Vis spectra and tested in formaldehyde photodegradation. The results indicated some synergy between ZnS and Fe_2O_3, resulting in slightly higher catalytic activity of ZnS/Fe_2O_3 than idividual ZnS and Fe_2O_3. The order of photoactivity of the synthesized particles was ZnS/Fe_2O_3 > ZnS > Fe_2O_3.

REFERENCES

1. Mills, A. and Hunte, S L., *J. Photochem. Photobiol. A: Chem.*, 1997, vol. 108, p. 1.
2. Hara, M., Hasei, H., Yashima, M., Ikeda, S., Takata, T., Kondo, J.N., and Domen, K., *Appl. Catal. A: General*, 2000, vol. 190, p. 35.
3. Zheng, L.R., Zheng, Y.H., Chen, C.Q., Zhan, Y.Y., Lin, X.Y., Zheng, Q., Wei, K.M., and Zhu, J.F., *Inure Chem*., 2009, vol. 48, p. 1819.
4. Pal, B., Sharon, M., and Nogami, G., *Mater. Chem. Phys*., 2009, vol. 59, p. 254.
5. Hameed, A., Montini, T., Gonbac, V., and Fornasiero, P., *Photochem. Photobiol. Sci.,* 2009, vol. 8, p. 677.
6. Bessekhouad, Y., Robert, D., and Weber, J.V., *Catal. Today*, 2005, vol. . 101, p. 315.
7. Shah, P., Siddhapara, K.S., and Shah, D.V., *Carbon-Science and Technology, Applied Science Innovations*, 2013, vol. 5/2, pp. 303–308.
8. Shchukin, D.G. and Caruso, R.A., *Chem. Mater.*, 2004, no. 16, p. 2287.
9. Gurr, J.R., Wang, A.S., Chenand, C.H., and Jan, K.Y., *Toxicology.* 2005, vol. 213, p. 66.
10. Tambweker, S.V., Venugopal, D., and Subrahmanyam, M., *Int. J. Hydrogen Energy*, 1999, vol. 24, p. 957.
11. Pooja, S.L., Satyajyoti, S., Kumar, R., and Narendra, M.G., *Int. J. Hydrogen Energy*, 2007, vol. 32, p. 2784.
12. Priya, R. and Kanmani, S., *Solar Energy*, 2009, vol. 83, p. 1802.
13. Linkous, C.A., Muradov, N.Z., and Ramser, S.N., *Int. J. Hydrogen Energy*, 1995, vol. 20, p. 701.
14. Davidson, W.L., *Phys. Rev*., 1948, vol. 74, p. 116.
15. Shi, Z.L., Ce Du, and Shu-Hua Yao, *J. Taiwan. Inst. Chem. Eng.*, 2011, vol. 42, p. 652.
16. Preethi, V. and Kanmani, S., *Int. J. Hydrogen Energy*, 2014, vol. 39, p. 1613.
17. Ding, Z., Lu, G.Q., and Greenfield, P.F., *J. Phys. Chem. B*, 2000, vol. 104, p. 4815.
18. Marc, G., Augugliaro, V., López-Muñoz, M.J., Martın, C., Palmisano, L., Rives, V., Schiavello, M., Tilley, R.J.D., and Venezia, A.M., *J. Phys. Chem. B*, 2001, vol. 105, p. 1033.
19. Herrmann, J.M., *Catal. Today*, 1999, vol. 53, p. 115.